DOI: 10.1002/ejic.200701303

Synthesis and Characterisation of Poly(bipyridine)ruthenium Complexes as Building Blocks for Heterosupramolecular Arrays

Matthias Schwalbe,[a] Bernhard Schäfer,[a] Helmar Görls,[a] Sven Rau,*[a] Stefanie Tschierlei,[b] Michael Schmitt,[b] Jürgen Popp,[b] Gavin Vaughan,[c] William Henry,[d] and Johannes G. Vos[d]

Keywords: Ruthenium / Bipyridine / Microwave-assisted reaction / Raman spectroscopy

Poly(bipyridine)ruthenium complexes with carboxylate anchor groups are key components in dye-sensitised solar cells. In this contribution, an improved microwave-assisted synthetic procedure is presented for the important building block $[RuCl_2(dcmb)_2]$ (dcmb = 4,4′-dimethoxycarbonyl-2,2′-bipyridine), which results in short reaction times and high purity. The methyl esters are easily deprotected to give free carboxylate functions. In addition, a full structural, spectral and electrochemical characterisation of a series of complexes with the general formula $[Ru(dcmb)_{3-n}(tbbpy)_n](PF_6)_2$ with n = 0–3 and tbbpy = 4,4′-di-*tert*-butyl-2,2′-bipyridine is presented. The location of the lowest-energy metal-to-ligand charge transfer (MLCT) excited state is investigated by resonance Raman spectroscopy for selected complexes. The results obtained indicate that the nature of the excited state that is populated is dependent on the excitation wavelength.

Introduction

Over the last 20 years poly(bipyridine)ruthenium complexes have been extensively studied because of their exceptional photochemical properties.[1] In particular, their ability to function as tuneable pigments in dye-sensitised solar cells (dssc) has attracted considerable attention. Grätzel et al. and other groups reported that complexes with carboxylate anchor groups bind strongly to the titanium dioxide surface of such solar cells.[2] The majority of the complexes investigated utilise 4,4′-dicarboxy-2,2′-bipyridine as the anchoring ligand. It has been shown that this ligand facilitates photoinduced electron transfer from the excited ruthenium centre to the surface, which is crucial for the efficiency of dssc devices.[3]

In addition to their application in solar cells,[9] the attachment of ruthenium complexes to surfaces allows for a range of other potential applications ranging from sensors[4] to photocatalysis,[5] molecular switches,[6] electromechanical motors[7] or light-collecting molecular antenna.[8] A number of chemical properties are important for the application of surface-bound complexes. For instance, their long-life stability relies on a stable redox system, like the Ru^{II}/Ru^{III} couple, and a stable bond between pigment and surface, which has indeed been observed for carboxylate functions. The strength of the binding of the ruthenium complexes increases with increasing number of anchoring groups per molecular unit. Unfortunately, the synthesis and, in particular, the purification of metal complexes with multiple carboxylate functions is very challenging, and the availability of efficient synthetic pathways towards the required functional building blocks is an important issue. Previously, we have shown that poly(bipyridine)ruthenium complexes containing 2,2′-bipyridine (bpy), 4,4′-dimethyl-2,2′-bipyridine (dmbpy) and 4,4′-di-*tert*-butyl-2,2′-bipyridine (tbbpy) can be prepared in high yields of up to 95% by microwave-assisted reactions.[10] In this contribution, we describe the extension of this methodology to the synthesis of a series of ruthenium complexes containing up to six carboxylate anchoring groups. By using appropriate protecting groups, improved yields and reduced reaction times are observed.

We have utilised two different ligands to prepare a series of model complexes and to evaluate the synthetic flexibility of the methodology. In addition, the influence of the introduction of dimethoxycarbonyl-based ligands on the chemical and photophysical properties is investigated. The ligands 4,4′-dimethoxycarbonyl-2,2′-bipyridine (dcmb) and 4,4′-di-*tert*-butyl-2,2′-bipyridine (tbbpy) are used to prepare the complexes $[Ru(dcmb)_{3-n}(tbbpy)_n](PF_6)_2$ with n = 0–3 (**2**, **3**, **4**, **5**), as shown in Figure 1. The latter ligand, i.e. tbbpy, induces solubility in less polar solvents, whereas the former can easily be deprotected and bound to TiO_2 surfaces. As

[a] Institute of Inorganic and Analytical Chemistry, FSU – Jena, August-Bebel-Str. 2, 07743 Jena, Germany
Fax: +49-3641-948102
E-mail: sven.rau@uni-jena.de
[b] Institute of Physical Chemistry, FSU – Jena, Helmholtzweg 4, 07743 Jena, Germany
[c] European Synchrotron Radiation Facility (ESRF), B. P. 220, 38043 Grenoble Cedex, France
[d] National Centre for Sensor Research, School of Chemical Sciences, Dublin City University, Dublin 9, Ireland

it is very important to know the location of the excited state for a rational design of photo- and redox active compounds, we investigated them using resonance Raman spectroscopy. The results indicate that the nature of the excited state that is populated in the heteroleptic complexes is dependent on the excitation wavelength.

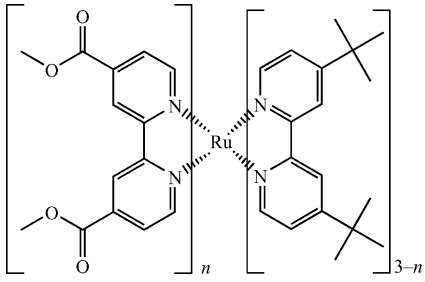

Figure 1. Structure of the synthesised complexes.

A similar series of complexes with the general formula $[Ru(decbpy)_n(dmbpy)_{3-n}](PF_6)_2$ with n = 0–3, decbpy = diethoxycarbonylbipyridine and dmbpy = dimethylbipyridine was prepared by Schmehl et al.[11] On the basis of a combination of absorption, emission and electrochemical measurements, Schmehl et al. suggested that the highest-occupied molecular orbital (HOMO) for $[Ru(decbpy)_3]^{2+}$ is lowest in energy relative to those of the other compounds in the series. With an increasing number of dmbpy ligands, an increase in the energy of this orbital was postulated. However, no solid-state structures or resonance Raman data are presented in this publication to support this interpretation. To the best of our knowledge, we present here the most efficient synthetic procedure for the preparation of dyes for dye-sensitised solar cells, in conjunction with the first complete structurally and photochemically investigated series of complexes of that kind.

Results and Discussion

Synthesis of the Ruthenium Complexes

4,4′-Dimethoxycarbonyl-2,2′-bipyridine (dcmb) was prepared starting from 4,4′-dimethyl-2,2′-bipyridine, which can be oxidised with either $KMnO_4$ (70% yield)[12] or $K_2Cr_2O_7$ as the oxidising agent. The latter gave better yields of the dicarboxy compound (90%) as was seen previously,[13] and we therefore used this method. The subsequent protection of the acid as the methyl ester gives the desired ligand in an overall yield of 60% (starting from the dimethyl analogue). Protection was carried out as the presence of free carboxylate functions would induce severe problems in the workup of the desired complexes, as these compounds start to behave similarly to surfactants. Furthermore, the synthesis of such ruthenium complexes containing free carboxylate functions requires harsh conditions and the use of pressure vessels, as shown by Pakkanen et al.[14] It is highly likely that multiple protonation/deprotonation reactions play a detrimental role and lead to limiting yields and prolonged reaction times. The synthesis of heteroleptic poly(bipyridine) compounds of this type generally starts with the preparation of a ruthenium dichloride as the building block, in this case $[RuCl_2(dcmb)_2]$ (**1**). This compound can be prepared almost in the same manner as that previously reported for $[RuCl_2(tbbpy)_2]$[10] by using microwave irradiation in dry DMF with 2 equiv. dcmb and $[RuCl_2(cod)]_n$ in less than 2 h. This is a significant advantage compared to the long (50 h) and lower yielding (78%) thermal reaction.[15] Compound **1** is obtained in over 95% purity after a brief workup procedure – removal of DMF from the reaction solution, dissolution of the crude product in chloroform and precipitation by addition of diethyl ether. No further purification by column chromatography is required; see Figure 2 for the ^1H NMR spectrum of the reaction product. This is the first time that compound **1** has been prepared in a fast reaction procedure giving high purity and high

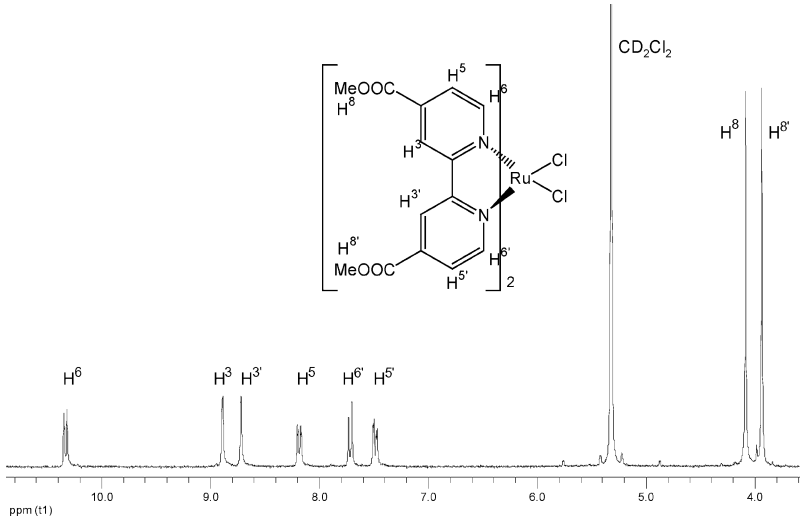

Figure 2. ^1H NMR spectrum of $[RuCl_2(dcmb)_2]$ (**1**) in CD_2Cl_2.

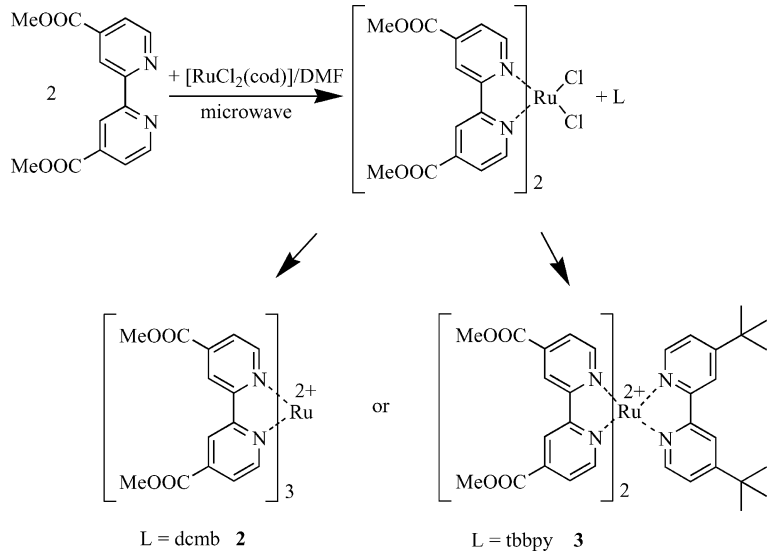

Scheme 1. Synthesis of the compounds **1**, **2** and **3**.

yield. The efficient access to complex **1** reported here is of significant importance as **1** represents an essential building block in dye-sensitised solar cell architectures.

The syntheses of $[RuCl_2(dcmb)_2]$ (**1**), $[Ru(dcmb)_3](PF_6)_2$ (**2**) and $[Ru(dcmb)_2(tbbpy)](PF_6)_2$ (**3**) are shown in Scheme 1. Ligand substitution to prepare compounds **2** and **3** was performed in refluxing methanol/water in order to avoid high temperatures, which could lead to decarboxylation. All reactions can be performed in the microwave as well by using a methanol/water mixture. Previously, it was reported that decarboxylation can take place in such reactions when sealed tubes in a microwave oven were used.[16] This was not observed in our case where we use a pressureless setup. After removal of methanol, the aqueous solution is filtered to remove excess ligand. Upon addition of NH_4PF_6, the desired product is formed as a red precipitate, which can be isolated and washed with diethyl ether.

The synthetic approach towards $[Ru(dcmb)(tbbpy)_2](PF_6)_2$ (**4**) and $[Ru(tbbpy)_3](PF_6)_2$ (**5**) is similar, but starts from $[RuCl_2(tbbpy)_2]$.

The introduction of the methyl protecting groups for the carboxylate functions increases the solubility of the formed complexes, simplifies workup and improves the yield. With the ester groups, the solubility is very good in acetonitrile, acetone and is also good in dichloromethane, whereas complexes with more than two free carboxylate functions per ruthenium centre become insoluble in these solvents. No column chromatography was needed for purification of the obtained complexes. This is another important feature of the high yield and high purity preparation developed here, as ester functionalities in ruthenium complexes tend to decompose during chromatographical workup, which diminishes yields and purity.

However, the attachment of ruthenium complexes to TiO_2 surfaces requires the presence of free carboxylate groups. The free carboxylate functions are obtained when the ester compound is stirred in an aqueous solution of sodium hydroxide or sodium carbonate for several hours, as described in the Experimental Section. The corresponding sodium salt can be isolated in reasonable yields by precipitation with ethanol or tetrahydrofurane. The sodium salts show slight solubility in methanol or DMF, from which a fixation to titanium dioxide surfaces is possible.

Structures of the Ruthenium Complexes

Crystals suitable for single-crystal X-ray analysis were obtained for compound **1** upon slow evaporation of an acetonitrile/toluene solution containing the compound. Figure 3 shows an octahedrally coordinated ruthenium centre, and the two chlorido ligands are in a *cis* arrangement.[17] No exchange of chlorido ligands with acetonitrile was observed.

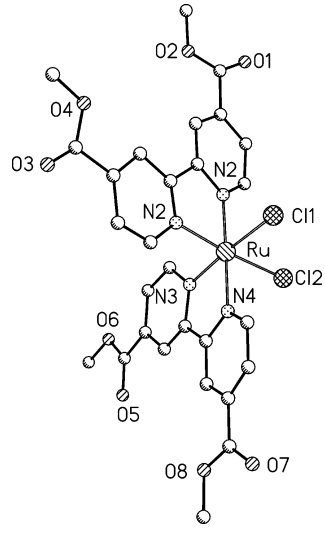

Figure 3. Structural motif of compound **1**.

Complexes **2**– **5** were recrystallised from acetone/water/methanol solutions. The solid-state structures of compounds **2**–**5** are presented in Figures 4, 5, 6 and 7, relevant bond lengths and angles can be found in the captions.

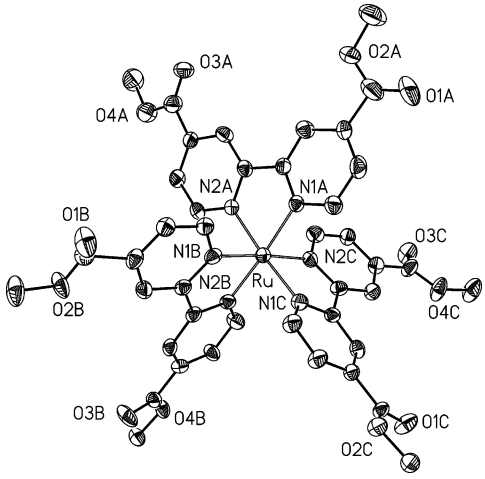

Figure 4. Molecular structure of complex **2** (H atoms and PF_6 ions are omitted for clarity). Selected bond lengths [Å] and bond angles [°]: Ru–N1A 2.061(6), Ru–N1B 2.041(7), Ru–N2A 2.049(6), Ru–N2B 2.048(7), Ru–N1C 2.056(7), Ru–N2C 2.067(6), N1A–Ru–N2B 175.7(2), N1B–Ru–N2C 175.4(3), N2A–Ru–N1C 175.7(2), N1A–Ru–N2A 78.6(2), N1B–Ru–N2B 78.9(2), N1C–Ru–N2C 79.1(3).

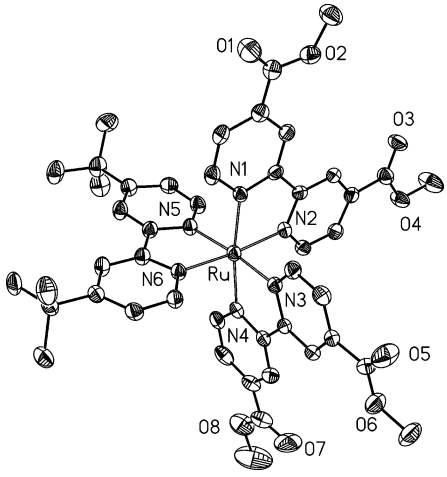

Figure 5. Molecular structure of complex **3** (H atoms and PF_6 ions are omitted for clarity). Selected bond lengths [Å] and bond angles [°]: Ru–N1 2.055(4), Ru–N2 2.059(4), Ru–N3 2.056(4), Ru–N4 2.052(4), Ru–N5 2.059(4), Ru–N6 2.058(4), N1–Ru–N4 172.05(16), N2–Ru–N6 174.64(16), N3–Ru–N5 173.84(16), N1–Ru–N2 78.63(16), N3–Ru–N4 79.16(17), N5–Ru–N6 78.41(16).

All tris(bipyridine) complexes have a similar basic structure of a distorted octahedrally coordinated ruthenium centre. The Ru–N bond lengths vary between 2.041(7) and 2.068(5) Å, and the N–Ru–N bite angles of the bipyridines vary between 77.92(19)° and 79.3(2)°. No trends in the Ru–N distances and the N–Ru–N angles are observed. The effect of the methoxycarboxylate substituents in the periphery of the complexes on the structural parameters around the ruthenium centre is negligible. For example, no *trans* effect is observed, and the variation in the bond lengths can be attributed to vibrational effects. The N–Ru–N angles deviate greatly from the ideal 90° value, but this fact is due to the small bite angle of the bipyridines and agrees well with known structural parameters in the literature.[14,18] The distortion of the octahedron stems, very likely, from the combination of bite angle and repulsion of the ligands.

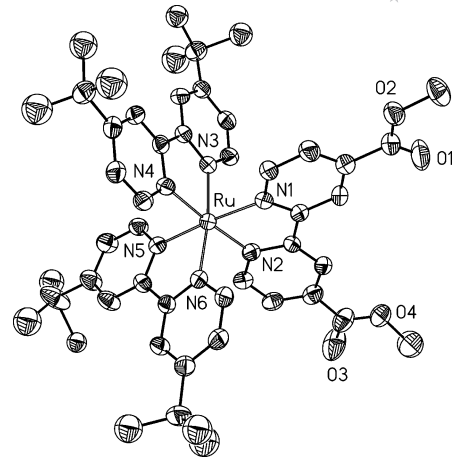

Figure 6. Molecular structure of complex **4** (H atoms and PF_6 ions are omitted for clarity). Selected bond lengths [Å] and bond angles [°]: Ru–N1 2.068(5), Ru–N2 2.054(5), Ru–N3 2.061(5), Ru–N4 2.063(5), Ru–N5 2.052(5), Ru–N6 2.046(5), N1–Ru–N5 174.95(19), N2–Ru–N4 175.70(19), N3–Ru–N6 172.30(18), N1–Ru–N2 79.3(2), N3–Ru–N4 78.19(19), N5–Ru–N6 77.92(19).

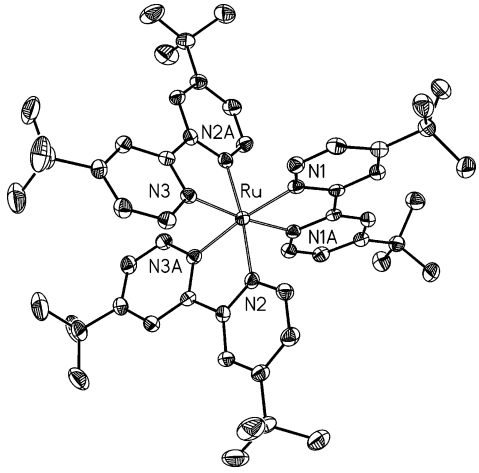

Figure 7. Molecular structure of complex **5** (H atoms and PF_6 ions are omitted for clarity). Selected bond lengths [Å] and bond angles [°]: Ru–N1A 2.055(3), Ru–N1 2.055(3), Ru–N2A 2.062(3), Ru–N2 2.062(3), Ru–N3A 2.063(3), Ru–N3 2.063(3), N1A–Ru–N1 78.64(14), N3A–Ru–N2 78.39(10), N2A–Ru–N3 78.39(10), N1A–Ru–N3 172.43(10), N1–Ru–N3A 172.43(10), N2A–Ru–N2 173.24(14).

Spectroscopic Properties of the Compounds

All spectroscopic investigations were performed in dichloromethane and acetonitrile. There are slight differences between the UV/Vis spectra in the two different solvents because of the different polarity of the solvent. These

Table 1. Absorption and emission maxima in dichloromethane and acetonitrile; extinction coefficients are given in parentheses [$M^{-1}\,cm^{-1}$].

Complex	λ_{max} [nm] (CH_2Cl_2)	λ_{max} [nm] (CH_3CN)	λ_{em} [nm] (CH_2Cl_2)	λ_{em} [nm] (CH_3CN)	τ [ns] (aerated CH_3CN)	τ [ns] (deaerated CH_3CN)	τ [ns] (aerated CH_2Cl_2)
5 $[Ru(tbbpy)_3](PF_6)_2$	461 (15700)	458 (16000)	604	613	107	730	248
2 $[Ru(dcmb)_3](PF_6)_2$	464 (23400)	467 (19700)	619	631	603	1174	992
3 $[Ru(dcmb)_2(tbbpy)](PF_6)_2$	442, 485 (16200, 18600)	443, 486 (14300, 16900)	645	657	395	1002	678
4 $[Ru(dcmb)(tbbpy)_2](PF_6)_2$	425, 494 (12900, 12800)	426, 492 (11400, 11000)	681	691	229	646	448

differences are, however, far less pronounced when compared with data obtained for some ruthenium complexes with tetrasubstituted phenanthrolines.[19] In addition, the emission is stronger in dichloromethane than in acetonitrile, and the maxima observed are blueshifted by approximately 10 nm for dichloromethane.

The absorption spectra of the homoleptic compounds **2** and **5** in dichloromethane show a single maximum at 464 nm and 461 nm, respectively. The heteroleptic compounds **3** and **4** show two maxima in the region between 400 and 500 nm (see Table 1), which can be assigned to the two possible MLCT states of the two different ligands, corresponding to a transition from the d orbital of the ruthenium centre to the π* orbital of tbbpy or dcmb. Absorption spectra of the complexes $[Ru(dcmb)_{3-n}(tbbpy)_n](PF_6)_2$ with $n = 0–3$ in dichloromethane are shown in Figure 8. The shift in the absorption maxima in the case of the heteroleptic compounds probably occurs as a result of a decrease in symmetry and a cumulative effect of electron-withdrawing and electron-donating properties.[11]

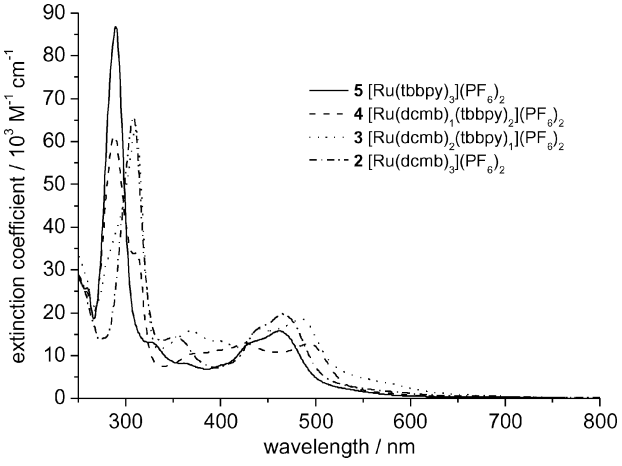

Figure 8. Absorption spectra of the series of complexes $[Ru(dcmb)_{3-n}(tbbpy)_n](PF_6)_2$ with $n = 0–3$ in dichloromethane solution.

The emission spectra of the complexes show a single maximum in the region between 600 and 700 nm (Figure 9). The order (in nm) of the emission maxima is **4** > **3** > **2** > **5**, which corresponds to the order (in nm) of the absorption maxima, as is expected for the photophysical deactivation processes in such systems. The emission most likely occurs exclusively from the lowest lying ^{3}MLCT state.

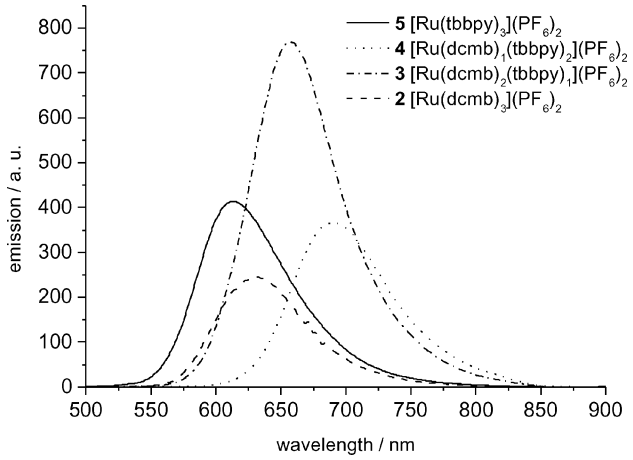

Figure 9. Emission spectra of the series of complexes $[Ru(dcmb)_n(tbbpy)_{3-n}](PF_6)_2$ with $n = 0–3$ in acetonitrile solution.

The lifetime measurements for the series of compounds $[Ru(dcmb)_{3-n}(tbbpy)_n](PF_6)_2$ with $n = 0–3$ were performed in aerated or deaerated acetonitrile and dichloromethane (Table 1). For all the compounds, the values obtained are higher in dichloromethane than in acetonitrile. The smallest increase is observed for compound **2**; in this case, the lifetime of the excited state in dichloromethane is only increased by 50%. As expected, the lifetimes are also higher in deaerated solvents than in aerated solvents. With increasing numbers of dcmb ligands, the lifetimes increase too. Interestingly, compound **2** presents the highest lifetime of the four complexes, and the value exceeds 1 μs in deaerated acetonitrile. The increase in lifetime for compound **5** on going from aerated to deaerated solvents renders this complex a potential candidate for luminescent oxygen sensing.[19]

Resonance Raman Data of the Complexes

To obtain further information on the location of the ^{1}MLCT excited state, compounds **2**, **4** and **5** were investigated by resonance Raman spectroscopy. The location of the excited state is especially important in metal complexes that serve as dyes in dye-sensitized solar cells. If the excited state is not located on the TiO_2-bound ligand, lower efficiencies of charge injection are observed.[9] To the best of our knowledge, the results presented here are the first reso-

nance Raman spectroscopy experiments done on a complete series of complexes with carboxylate functions.

All resonance Raman spectra were measured in dichloromethane. The nonresonant Raman spectra of the solids of the homoleptic compounds **2** and **5** presented marker bands that can be assigned to one specific ligand, i.e. tbbpy (**5**) or dcmb (**2**). From the nonresonant Raman spectra, the peaks at 1731, 1549, 1474 and 1445 cm^{-1} can be associated with the dcmb ligand and the peaks at 1486 and 1422 cm^{-1} to the tbbpy ligand. The peaks at 1617, 1320, 1028 and 1032 cm^{-1} cannot be assigned to one specific ligand because of overlaps (see Table 2).

Table 2. Summary of the Raman bands of the free ligands tbbpy and dcmb as well as of the complexes $[Ru(tbbpy)_3](PF_6)_2$ (**5**), $[Ru(dcmb)(tbbpy)_2](PF_6)_2$ (**4**) and $[Ru(dcmb)_3](PF_6)_2$ (**2**) in the nonresonant Raman experiment; excitation wavelengths are given in parentheses [nm] and wavenumbers in cm^{-1}.

tbbpy (830.15)	**5** (830.15)	**4** (830.15)	**2** (1064)	dcmb (830.15)
		1731	1732	1729
1609	1614	1617	1617	1604
		1549	1553	1565
1552	1537			
1491	1480	1486		
		1474	1474	1437
		1445	1447	1427
1426	1417	1422		
1321	1313	1320	1324	1324
1001	1027	1028+1032	1029	997

The excitation wavelength for the resonance Raman experiments was 488 nm or 457 nm, which was obtained with a continuous wave argon-ion laser. The excitation wavelength for compound **5**, 457 nm, is close to the absorption maxima at 466 nm, and all enhanced peaks (1615, 1538, 1481, 1317 and 1031 cm^{-1}) can be assigned to a d–π* transition from ruthenium to tbbpy as previously reported (see Figure 10).[20] The excitation wavelength for compound **2** was also 457 nm and close to the absorption maxima at 461 nm, and all enhanced peaks (1737, 1619, 1553, 1477, 1448, 1323 and 1025 cm^{-1}) can be assigned to a d–π* transition from ruthenium to dcmb.

In case of the heteroleptic complex **4** d–π*-transitions to both ligands are possible as indicated by the absorption spectra. The resonance enhancement depends on the location of the MLCT process, which is activated with the excitation wavelength. The transition to either a tbbpy or a dcmb ligand or to both ligands simultaneously may occur. For the absorption maxima at 492 nm, which is lowest in energy, the excitation wavelength is 488 nm. This resonance Raman spectrum shows a good agreement with the spectrum for **2**, i.e. for the homoleptic dcmb compound.

For the second absorption maxima at 424 nm, we used an excitation wavelength of 457 nm. Unfortunately, this value is not very close to the absorption maxima, because of restrictions of the laser wavelengths, and so still contains some part of the long wavelength absorption. This is very likely the reason why we can see an enhancement in both MLCTs in the spectrum; in particular, a peak at 1484 cm^{-1} and a shoulder at 1541 cm^{-1}, which we can assign to the

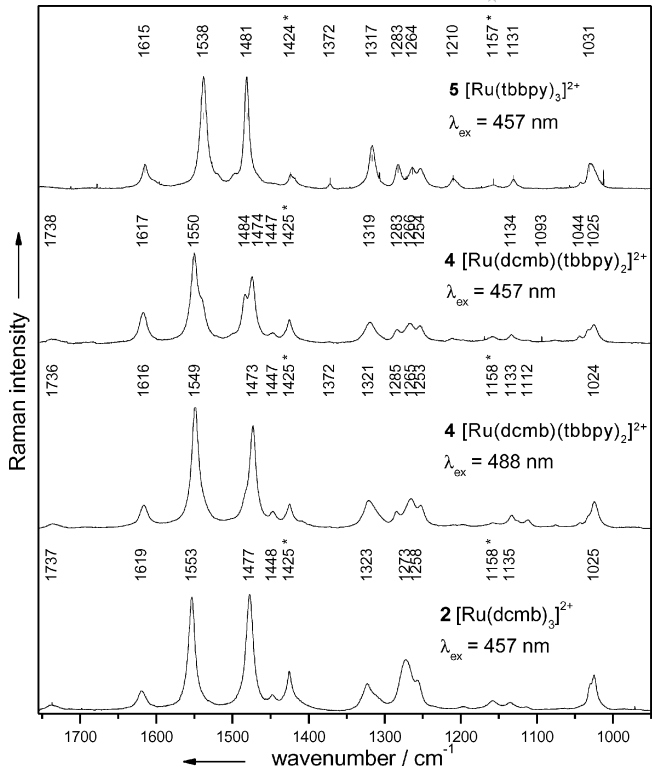

Figure 10. Resonance Raman spectra of $[Ru(tbbpy)_3](PF_6)_2$ (**5**), $[Ru(dcmb)(tbbpy)_2](PF_6)_2$ (**4**) and $[Ru(dcmb)_3](PF_6)_2$ (**2**) dissolved in dichloromethane. Peaks of the solvent are marked with an *; the spectrum of **4** is normalised relative to the solvent band at 1425 cm^{-1}.

ruthenium–tbbpy transition, arise in addition to the peaks for the ruthenium–dcmb transition.

Nonetheless, on the basis of the resonance Raman data obtained, we can assign the absorption maxima at 424 nm, at least partially, to a MLCT transition from the ruthenium centre to a tbbpy ligand, while the absorption at 492 nm can exclusively be assigned to a MLCT transition to a dcmb ligand. A "summarisation" of the ^{1}MLCT processes that occur in compounds **2**, **4** and **5** is presented in Figure 11, and these processes agree well with the electrochemical data reported below.

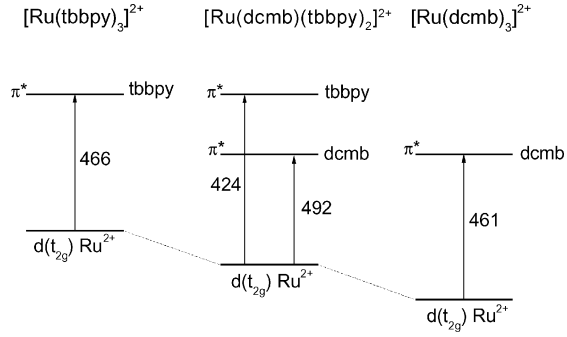

Figure 11. Schematic representation of the MLCT transitions of the different compounds **2**, **4** and **5**.

Electrochemistry

The oxidation and reduction potentials of all the complexes in the series $[Ru(dcmb)_n(tbbpy)_{3-n}](PF_6)_2$ with n = 0–3 and also the ΔE values for the potential difference between the first oxidation (E_{ox}) and the first reduction (E_{red1}) process are given in Table 3. All electrochemical processes appear to be quasireversible. In accordance to Schmehl et al.,[11] these values are linearly related to the absorption maxima. The electrochemical data show a decreasing order of the ΔE value from **5** > **2** > **3** > **4**, which corresponds to the order of the absorption maxima and so supports a linear relationship. The dcmb ligand, being a better π acceptor, shows two reduction processes. The data obtained suggest that, in the case of mixed-ligand complexes, the first ligand that is reduced is a dcmb ligand. Thereafter, a second dcmb ligand or a tbbpy ligand is reduced. Only when every other ligand is reduced can the dcmb ligand be reduced for a second time.

Table 3. Oxidation and reduction potentials for the series of complexes $[Ru(dcmb)_{3-n}(tbbpy)_n](PF_6)_2$ with n = 0–3 [potentials recorded in acetonitrile against ferrocene (0.47 V) as internal standard and tetrabutylammonium hexafluorophosphate as supporting electrolyte]; ΔE = potential difference between first oxidation and first reduction process.

Complex	E_{ox} [V]	E_{red1} [V]	E_{red2} [V]	E_{red3} [V]	E_{red4} [V]	E_{red5} [V]	E_{red6} [V]	ΔE [V]
5	0.73	–1.82	–2.02	–2.28				2.55
4	0.89	–1.40	–1.90	–2.12	–2.39			2.29
3	1.05	–1.32	–1.52	–1.99	–2.19	–2.48		2.37
2	1.18	–1.28	–1.44	–1.65	–2.10	–2.26	–2.54	2.46

Conclusions

In conclusion, we have shown that heteroleptic ruthenium complexes are easily accessible starting from $[RuCl_2(dcmb)_2]$ and $[RuCl_2(tbbpy)_2]$. Both starting compounds can be prepared in high yields and in short reaction times by using microwave-assisted reaction conditions. The introduction of another bipyridine ligand leads to the functional building blocks; this second step proceeds with reasonable yields. Characteristic for both steps, are the short reaction times of less than 2 h and the high purities of the obtained complexes. The solid-state structures of all compounds are similar and show distorted octahedrally coordinated ruthenium centres. In the series of complexes investigated, no correlation between the solid-state structures and the photophysical properties of the complexes is obtained. Absorption and emission maxima follow the order **4** > **3** > **2** > **5** and show highest extinction coefficients in dichloromethane. The same order can be found for the electrochemically measured ΔE values. The resonance Raman data show that the lowest-energy absorption maximum can be assigned to a MLCT transition from the ruthenium centre to a dcmb ligand, and thus verifies experimentally the hypothesis of Schmehl. This fact is important because it means that upon excitation of a ruthenium compound, the lowest lying π* orbital that is populated first is a carboxy-substituted bipyridine. On fixation to a titanium dioxide surface, the electron can be introduced from the ruthenium via the carboxylated bipyridine into the conduction band of the surface, which is the crucial step in the application as solar cell devices. Hence, the direction of the photoelectron transfer is predetermined by the choice of the connecting ligand. The influence of the connection of the complexes to TiO_2 will be part of following studies.

Experimental Section

^1H NMR and ^{13}C NMR spectra were recorded at ambient temperature with a Bruker AC 200 or AC 400 MHz spectrometer. All spectra were referenced to TMS or deuterated solvent as an internal standard. Mass spectra were recorded with a MAT 95 XL or a SSQ 170, Finnigan Mat. The positive ES mass spectra were obtained with voltages of 3–4 kV applied to the electrospray needle. IR measurements were carried out with a Perkin–Elmer System 2000 FT-IR. UV/Vis absorption spectra (accuracy ±2 nm) were obtained with a Specord S 600 (AnalytikJena) with standard software-based tools. Emission spectra (accuracy ±5 nm) were measured at 298 K by using a Perkin–Elmer LS50B luminescence spectrophotometer equipped with a Hamamatsu R928 red-sensitive detector. Emission spectra are uncorrected for photomultiplier response. 10-mm path length quartz cells were used for recording spectra. Luminescence lifetime measurements were obtained with an Edinburgh Analytical Instruments (EAI) time-correlated single photon counting apparatus (TCSPC) comprising two model J-yA monochromators (emission and excitation), a single photon photomultiplier detection system model 5300 and a F900 nanosecond flashlamp (nitrogen filled at 1.1 atm pressure, 40 kHz or 0.3 atm pressure, 20 kHz) interfaced with a personal computer by a NorlandMCA card. A 410-nm cut-off filter was used in emission to attenuate scatter of the excitation light (337 nm); luminescence was monitored at the k_{max} of the emission. Data correlation and manipulation was carried out with EAI F900 software version 6.24. Samples were deaerated by using argon for 30 min prior to measurements, followed by repeated purging to ensure complete oxygen exclusion. Emission lifetimes were calculated by using a single-exponential fitting function, Levenberg–Marquardt algorithm with iterative deconvolution (Edinburgh Instruments F900 software). The reduced $v2$, and residual plots were used to judge the quality of the fits. Lifetimes are ±5%. The resonance Raman spectra were obtained by using a continuous-wave argon-ion laser from Spectra Physics as the excitation source and a CCD-camera Photometrics M9000 as the detector. The electrochemical measurements were executed with a PGSTAT booth (manufacturer: Autolab) with the aid of the appropriate GPES software. The experiments were carried out by means of a three-electrode technique in degassed acetonitrile with tetrabutylammoniumtetrafluoroborate (0.1 M^{-1}) as the conducting salt. An Hg-dropping electrode or a rotating-disc platinum electrode was used as the working electrode. The reference electrode was an Ag/AgCl electrode. The calibration of the electrode took place according to the ferrocene standard potential in acetonitrile for which a value of +0.827 V was assumed. The microwave-assisted reactions were carried out with a Microwave Laboratory System MLS EM-2 microwave system. $RuCl_3 \cdot xH_2O$, NH_4PF_6, 4,4′-dimethyl-2,2′-bipyridine and all solvents were of commercial grade and used without further purification. $[RuCl_2(cod)]_n$,[21] 4,4′-ditertbutyl-2,2′-bipyridine (tbbpy)[22] and $[RuCl_2(tbbpy)_2]$ were prepared as described in the literature.

4,4′-Dicarboxy-2,2′-bipyridine (dcbpy): The ligand was prepared by using a variation of the known synthesis.[13] 4,4′-Dimethyl-2,2′-bipyridine (2.7 g, 15 mmol) was dissolved in concentrated sulfuric acid (70 mL). At 0 °C potassium dichromate (17.6 g, 60 mmol) was added in small portions. After that the reaction mixture was heated to 50 °C for 1 h. The green solution was poured into ice water (300 mL); the resulting precipitate was collected on a filter and washed with water until the filtrate became colourless. The pale green–yellow solid was refluxed in nitric acid (70 mL; 50% aq.) for 4 h, poured into 300 mL ice, filtered and washed with water and acetone. The resulting white solid was dried in vacuo. Yield: 3.16 g (86%). $C_{12}H_8N_2O_4$ (244.2): calcd. C 59.02, H 3.30, N 11.47; found C 58.72, H 3.25, N 11.43. IR (KBr): $\tilde{\nu}$(C=O) = 1721 (s) cm^{-1}. MS (EI): *m*/*z* (%) = 244 (40) $[M]^+$, 200 (100) $[M - CO_2]^+$, 172, 155. ^{1}H NMR (200 MHz, D_2O/Na, 300 K): δ = 8.56 (dd, *J* = 0.8, 5.0 Hz, 2 H), 8.17 (dd, *J* = 0.8, 1.6 Hz, 2 H), 7.65 (dd, *J* = 1.6, 5.0 Hz, 2 H) ppm.

4,4′-Dimethoxycarbonyl-2,2′-bipyridine (dcmb): The ligand was prepared as described in the literature.[23] $C_{14}H_{12}N_2O_4$ (272.25). IR (KBr): $\tilde{\nu}$(C=O) = 1732 (s) cm^{-1}. MS (EI): *m*/*z* (%) = 272 (20) $[M]^+$, 241 (10) $[M - CH_3O]^+$, 214 (100) $[M - CH_3OCO]^+$. ^{1}H NMR (200 MHz, $CDCl_3$, 300 K): δ = 8.94 (dd, J = 0.8, 1.6 Hz, 2 H), 8.84 (dd, J = 0.8, 5.0 Hz, 2 H), 7.87 (dd, J = 1.6, 5.0 Hz, 2 H), 3.96 (s, 6 H) ppm.

[RuCl$_2$(dcmb)$_2$] (1): The complex was prepared in an analogous fashion to [RuCl$_2$(tbbpy)$_2$].[10] A suspension of [RuCl$_2$(cod)]$_n$ (0.56 g, 2.0 mmol) and dcmb (1.09 g, 4.0 mmol) in DMF (150 mL) were treated for 1 h under microwave irradiation (microwave setup: 30 s, 600 W; 60 min, 200 W; 10 min, ventilation). The solvent was immediately removed with the rotary evaporator. The obtained dark green solid was recrystallised with chloroform/diethyl ether and dried in air. Yield: 1.29 g (90%). $C_{28}H_{24}Cl_2N_4O_8Ru{\cdot}H_2O$ (734.49): calcd. C 45.78, H 3.57, N 7.63; found C 45.81, H 3.48, N 7.69. IR (KBr): $\tilde{\nu}$(C=O) = 1725 (s) cm^{-1}. UV (methanol): λ_{max} = 555 nm. MS (ES in methanol): *m*/*z* (%) = 681 (20) $[M - Cl]^+$, 739 (100) $[M + Na]^+$, 1457 (40) $[2M + Na]^+$. ^{1}H NMR (400 MHz, CD_2Cl_2, 300 K): δ = 10.33 (dd, *J* = 0.4, 6.0 Hz, 2 H), 8.89 (dd, *J* = 0.4, 1.6 Hz, 2 H), 8.72 (dd, *J* = 0.4, 1.6 Hz, 2 H), 8.19 (dd, *J* = 1.6, 6.0 Hz, 2 H), 7.72 (dd, *J* = 0.4, 6.0 Hz, 2 H), 7.49 (dd, *J* = 1.6, 6.0 Hz, 2 H), 4.07 (s, 6 H), 3.93 (s, 6 H) ppm. ^{13}C{^{1}H} NMR (100 MHz, CD_2Cl_2, 300 K): δ = 53.1, 53.3, 122.1, 122.3, 124.7, 125.3, 135.2, 136.4, 153.1, 155.2, 158.6, 160.8, 164.5, 165.0 ppm. Crystals suitable for X-ray diffraction were obtained from a solution of acetonitrile/toluene.

[Ru(dcmb)$_3$](PF$_6$)$_2$ (2): A suspension of **1** (0.190 g, 0.265 mmol) and dcmb (0.072 g, 0.265 mmol) in methanol/water (40 mL/20 mL) was heated at reflux overnight. Methanol was removed with the rotary evaporator; the obtained solution was filtered, and an aqueous solution of NH_4PF_6 was added. The red-brown solid obtained was collected, washed with ethanol and diethyl ether and dried in air. Yield: 0.19 g (60%). $C_{42}H_{36}F_{12}N_6O_{12}P_2Ru{\cdot}H_2O$ (1225.76) calcd: C 41.15, H 3.12, N 6.86; found C 41.39, H 3.23, N 6.79. IR (KBr): $\tilde{\nu}$(C=O) = 1732 (s) cm^{-1}. UV (CH_3CN): λ_{max} = 467 nm. MS (ES in methanol): *m*/*z* (%) = 459 (90) $[(M - 2PF_6)/2]^{2+}$, 917 (50) $[M - 2PF_6 - H]^+$, 1063 (100) $[M - PF_6]^+$. ^{1}H NMR (400 MHz, CD_3CN, 300 K): δ = 9.05 (d, *J* = 1.6 Hz, 6 H), 7.86 (d, *J* = 6.0 Hz, 6 H), 7.82 (dd, *J* = 1.6, 6.0 Hz, 6 H), 3.98 (s, 18 H) ppm. ^{13}C{^{1}H} NMR (100 MHz, CD_3CN, 300 K): δ = 54.1, 125.1, 127.8, 140.5, 154.1, 158.3, 164.8 ppm. Crystals suitable for X-ray diffraction were obtained from a solution of acetone/water.

[Ru(dcmb)$_2$(tbbpy)](PF$_6$)$_2$ (3): A suspension of **1** (0.109 g, 0.152 mmol) and tbbpy (0.41 g, 0.152 mmol) in methanol/water (30 mL/20 mL) was heated at reflux overnight. Methanol was removed with the rotary evaporator; the obtained solution was filtered, and an aqueous solution of NH_4PF_6 was added. The red-brown solid obtained was collected, washed with ethanol and diethyl ether and dried in air. Yield: 0.10 g (55%). $C_{46}H_{48}F_{12}N_6O_8P_2Ru$ (1203.89): calcd. C 45.89, H 4.02, N 6.98; found C 45.77, H 4.07, N 6.75. IR (KBr): $\tilde{\nu}$(C=O) = 1732 (s) cm^{-1}. UV (CH_3CN): λ_{max} = 486 nm. MS (ES in methanol): *m*/*z* (%) = 457 (20) $[(M - 2PF_6)/2]^{2+}$, 913 (10) $[M - 2PF_6 - H]^+$, 1059 (100) $[M - PF_6]^+$. ^{1}H NMR (400 MHz, CD_2Cl_2, 300 K): δ = 8.99 (d, *J* = 1.6 Hz, 2 H), 8.98 (d, *J* = 1.6 Hz, 2 H), 8.28 (d, *J* = 2.0 Hz, 2 H), 8.02 (dd, *J* = 1.6, 6.0 Hz, 2 H), 7.96 (d, *J* = 6.0 Hz, 4 H), 7.91 (d, *J* = 6.0 Hz, 2 H), 7.53 (d, *J* = 6.0 Hz, 2 H), 7.48 (dd, *J* = 2.0, 6.0 Hz, 2 H), 4.03 (s, 6 H), 4.04 (s, 6 H), 1.41 (s, 18 H) ppm. ^{13}C{^{1}H} NMR (50 MHz, CD_2Cl_2, 300 K): δ = 30.3, 36.0, 53.7, 121.4, 123.9, 126.6, 127.9, 139.6, 151.2, 153.1, 156.2, 157.2, 157.5, 163.8, 163.9, 164.3 ppm. Crystals suitable for X-ray diffraction were obtained from a solution of acetonitrile/water/methanol.

[Ru(dcmb)(tbbpy)$_2$](PF$_6$)$_2$ (4): A suspension of [RuCl$_2$(tbbpy)$_2$] (0.142 g, 0.2 mmol) and dcmb (0.054 g, 0.2 mmol) in methanol/water (60 mL/20 mL) was heated at reflux overnight. Methanol was removed with the rotary evaporator; the obtained solution was filtered, and an aqueous solution of NH_4PF_6 was added. The red-brown solid obtained was collected, washed with ethanol and diethyl ether and dried in air. Yield: 0.18 g (75%). $C_{50}H_{60}F_{12}N_6O_4P_2Ru{\cdot}0.5H_2O$ (1209.04) calcd: C 49.67, H 5.09, N 6.95; found C 49.88, H 5.20, N 6.88. IR (KBr): $\tilde{\nu}$(C=O) = 1732 (s) cm^{-1}. UV (CH_3CN): λ_{max} = 492 nm. MS (ES in methanol): *m*/*z* (%) = 455 (10) $[(M - 2PF_6)/2]^{2+}$, 909 (10) $[M - 2PF_6 - H]^+$, 1055 (100) $[M - PF_6]^+$. ^{1}H NMR (400 MHz, CD_3CN, 300 K): δ = 9.02 (d, *J* = 1.6 Hz, 2 H), 8.48 (d, *J* = 2.0 Hz, 2 H), 8.46 (d, *J* = 1.6 Hz, 2 H), 7.90 (d, *J* = 6.0 Hz, 2 H), 7.82 (dd, *J* = 1.6, 6.0 Hz, 2 H), 7.53 (d, *J* = 6.0 Hz, 2 H), 7.50 (d, *J* = 6.0 Hz, 2 H), 7.42 (dd, *J* = 2.0, 6.0 Hz, 2 H), 7.34 (dd, *J* = 1.6, 6.0 Hz, 2 H), 3.99 (s, 6 H), 1.41 (s, 18 H), 1.39 (s, 18 H) ppm. ^{13}C{^{1}H} NMR (100 MHz, CD_3CN, 300 K): δ = 30.5, 36.4, 54.0, 122.7, 124.6, 125.7, 125.8, 127.4, 139.1, 151.7, 152.1, 153.6, 157.5, 157.6, 158.9, 164.2, 165.0 ppm. Crystals suitable for X-ray diffraction were obtained from a solution of acetone/water.

[Ru(tbbpy)$_3$](PF$_6$)$_2$ (5): The complex was prepared as described in the literature.[10] $C_{54}H_{72}F_{12}N_6P_2Ru$ (1196.17): calcd. C 54.22, H 6.07, N 7.03; found C 54.37, H 6.25, N 7.05. UV (CH_3CN): λ_{max} = 458 nm. MS (ESI in methanol): *m*/*z* (%) = 438 (10) $[(M - 2CH_3 - 2PF_6)/2]^{2+}$, 906 (10) $[M - 2PF_6 - H]^+$, 1051 (100) $[M - PF_6]^+$. ^{1}H NMR (200 MHz, CD_3CN, 300 K): δ = 8.52 (d, *J* = 2.0 Hz, 6 H), 7.54 (d, *J* = 6.0 Hz, 6 H), 7.38 (dd, *J* = 2.0, 6.0 Hz, 6 H), 1.94 (s, 18 H) ppm. ^{13}C{^{1}H} NMR (50 MHz, CD_3CN, 300 K): δ = 30.5, 36.3, 122.4, 125.6, 151.7, 157.9, 163.4 ppm. Crystals suitable for X-ray diffraction were obtained from a solution of acetone/water.

[Ru(dcbpy)$_3$]Na$_4$: A suspension of **2** (0.06 g, 0.05 mmol) with sodium hydroxide (0.014 g, 0.35 mmol) in water (20 mL) was heated at reflux overnight. The red solution was reduced in volume with the rotary evaporator; an orange precipitate was obtained on addition of ethanol. The solid was collected, washed with ethanol and diethyl ether and dried in air. The results obtained from the analysis of the compound agrees well with literature values.[24] Yield: 0.03 g (65%). IR (KBr): $\tilde{\nu}$(C=O) = 1607 (s) cm^{-1}. ^{1}H NMR (200 MHz, D_2O, 300 K): δ = 8.76 (d, *J* = 1.6 Hz, 6 H), 7.75 (d, *J* = 5.8 Hz, 6 H), 7.56 (dd, *J* = 1.6, 5.8 Hz, 6 H) ppm.

Crystal Structure Determination: The intensity data for the compounds were collected with a Nonius KappaCCD diffractometer, by using graphite-monochromated Mo-K_α radiation. For com-

pound **1**, measurements were carried out at beamline ID11 at the European Synchrotron Radiation Facility (ESRF). Data were collected with a Bruker Smart CCD-camera system at fixed 2θ, while the sample was rotated over 0.1° intervals over 2 s exposures, by using monochromated radiation from λ = 0.46409 Å. Data were corrected for Lorentz and polarisation effects, but not for absorption.[25–27] The structures were solved by direct methods (SHELXS[28]) and refined by full-matrix least-squares techniques against F_o^2 (SHELXL-97[29]). The hydrogen atoms of the structures were included at calculated positions with fixed thermal parameters. All non-hydrogen atoms were refined anisotropically.[29] The quality of the data for compound **1** was poor. Therefore, we will only publish the conformation of the molecule and the crystallographic data. We will not deposit the data in the Cambridge Crystallographic Data Centre. XP (Siemens Analytical X-ray Instruments, Inc.) was used for structure representations. CCSD-614182 (**2**), -614183 (**3**), -614184 (**4**), and -614185 (**5**) contain the supplementary crystallographic data for this paper. These data can be obtained free of charge from The Cambridge Crystallographic Data Centre via www.ccdc.cam.ac.uk/data_request/cif.

Crystal Data for 1: $C_{28}H_{24}Cl_2N_4O_8Ru$, Mr = 716.48 g mol^{-1}, green-brown prism, size 0.04 × 0.04 × 0.03 mm, triclinic, space group $P\bar{1}$, a = 13.4390(7), b = 13.6738(8), c = 15.8298(11) Å, α = 90.069(3), β = 90.022(3), γ = 89.995(3)°, V = 2908.9(3) Å^3, T = –90 °C, Z = 4, $\rho_{calcd.}$ = 1.636 g cm^{-3}, μ (λ = 0.46409 Å) = 4.15 cm^{-1}, F(000) = 1448, 25645 reflections in h(–18/18), k(–18/18), l(–21/21), measured in the range 1.68° ≤ Θ ≤ 18.80°, completeness Θ_{max} = 84.6%, 13793 independent reflections.

Crystal Data for 2: $C_{42}H_{36}F_{12}N_6O1_2P_2Ru{\cdot}0.5C_3H_6O$, Mr = 1236.82 g mol^{-1}, red-brown prism, size 0.05 × 0.05 × 0.04 mm, triclinic, space group $P\bar{1}$, a = 10.3660(4), b = 13.0534(5), c = 19.4694(9) Å, α = 94.930(2), β = 97.402(2), γ = 92.085(2)°, V = 2599.81(19) Å^3, T = –90 °C, Z = 2, $\rho_{calcd.}$ = 1.580 g cm^{-3}, μ (Mo-K_α) = 4.71 cm^{-1}, F(000) = 1248, 18434 reflections in h(–13/13), k(–16/16), l(–25/23), measured in the range 1.81° ≤ Θ ≤ 27.49°, completeness Θ_{max} = 98.4%, 11739 independent reflections, R_{int} = 0.049, 8444 reflections with $F_o > 4\sigma(F_o)$, 672 parameters, 0 restraints, R_{1obs} = 0.1249, wR_{2obs} = 0.3510, R_{1all} = 0.1617, wR_{2all} = 0.3763, GOOF = 1.428, largest difference peak and hole: 4.245/–2.058 e Å^{-3}.

Crystal Data for 3: $C_{46}H_{48}F_{12}N_6O_8P_2Ru{\cdot}1.5H_2O{\cdot}0.5CH_3CN$, Mr = 1251.46 g mol^{-1}, red-brown prism, size 0.06 × 0.06 × 0.04 mm, monoclinic, space group $P2_1/n$, a = 9.9092(2), b = 33.0889(7), c = 16.8815(4) Å, β = 98.440(1)°, V = 5475.2(2) Å^3, T = –90 °C, Z = 4, $\rho_{calcd.}$ = 1.518 g cm^{-3}, μ (Mo-K_α) = 4.45 cm^{-1}, F(000) = 2552, 32367 reflections in h(–12/9), k(–42/42), l(–21/21), measured in the range 2.17° ≤ Θ ≤ 27.48°, completeness Θ_{max} = 97.3%, 12192 independent reflections, R_{int} = 0.083, 6869 reflections with $F_o > 4\sigma(F_o)$, 710 parameters, 0 restraints, R_{1obs} = 0.0743, wR_{2obs} = 0.1767, R_{1all} = 0.1515, wR_{2all} = 0.2124, GOOF = 1.018, largest difference peak and hole: 1.605/–0.492 e Å^{-3}.

Crystal Data for 4: $C_{50}H_{60}F_{12}N_6O_4P_2Ru$, Mr = 1200.05 g mol^{-1}, red-brown prism, size 0.04 × 0.04 × 0.03 mm, monoclinic, space group $P2_1/n$, a = 18.6766(9), b = 16.0388(9), c = 19.9485(9) Å, β = 114.637(3)°, V = 5431.6(5) Å^3, T = –90 °C, Z = 4, $\rho_{calcd.}$ = 1.468 g cm^{-3}, μ (Mo-K_α) = 4.37 cm^{-1}, F(000) = 2464, 35699 reflections in h(–19/24), k(–20/20), l(–25/25), measured in the range 1.70° ≤ Θ ≤ 27.44°, completeness Θ_{max} = 99.3%, 12307 independent reflections, R_{int} = 0.050, 7837 reflections with $F_o > 4\sigma(F_o)$, 655 parameters, 0 restraints, R_{1obs} = 0.0878, wR_{2obs} = 0.2367, R_{1all} = 0.1367, wR_{2all} = 0.2773, GOOF = 1.038, largest difference peak and hole: 1.318/–1.112 e Å^{-3}.

Crystal Data for 5: $C_{57}H_{78}F_{12}N_6OP_2Ru$, Mr = 1254.26 g mol^{-1}, brown prism, size 0.38 × 0.32 × 0.30 mm, monoclinic, space group $C2/c$, a = 20.7485(7), b = 26.0046(7), c = 11.4949(4) Å, β = 103.392(2)°, V = 6033.5(3) Å^3, T = –90 °C, Z = 4, $\rho_{calcd.}$ = 1.381 g cm^{-3}, μ (Mo-K_α) = 3.93 cm^{-1}, F(000) = 2608, 8098 reflections in h(–23/22), k(–28/28), l(0/12), measured in the range 3.27° ≤ Θ ≤ 23.30°, completeness Θ_{max} = 94.8%, 4129 independent reflections, R_{int} = 0.054, 3564 reflections with $F_o > 4\sigma(F_o)$, 368 parameters, 0 restraints, R_{1obs} = 0.0465, wR_{2obs} = 0.1257, R_{1all} = 0.0572, wR_{2all} = 0.1332, GOOF = 1.017, largest difference peak and hole: 0.734/–0.886 e Å^{-3}.

Acknowledgments

We thank the Scholarship program of the Studienstiftung des Deutschen Volkes, the Deutsche Forschungsgemeinschaft, the Foundation for the technology, innovation and research in Thuringia (STIFT) for support of this research.

[1] V. Balzani, P. Piotrowiak, M. A. J. Rodgers, J. Mattay, D. Astruc, H. B. Gray, J. Winkler, S. Fukuzumi, T. E. Mallouk, Y. Haas, A. P. de Silva, I. Gould in *Electron Transfer in Chemistry*, Wiley-VCH, Weinheim, **2001**.
[2] B. O'Regan, M. Grätzel, *Nature* **1991**, *353*, 737–740; S. G. Yan, J. T. Hupp, *J. Phys. Chem. B* **1997**, *101*, 1493–1495; R. Hoyle, J. Sotomayor, G. Will, D. Fitzmaurice, *J. Phys. Chem. B* **1997**, *101*, 10791–10800; Y. Wang, J. B. Asbury, T. Lian, *J. Phys. Chem. A* **2000**, *104*, 4291–4299.
[3] a) X. Marguerettaz, D. Fitzmaurice, *J. Am. Chem. Soc.* **1994**, *116*, 5017–5018; b) K. Kalyanasundaram, M. Gratzel, *Coord. Chem. Rev.* **1998**, *177*, 347–414; c) G. Benko, J. Kallioinen, J. E. I. Korppi-Tommola, A. P. Yartsev, V. J. Sundstrom, *J. Am. Chem. Soc.* **2002**, *124*, 489–493; d) M. K. Nazeeruddin, P. Pechy, T. Renouard, S. M. Zakeeruddin, R. Humphry-Baker, P. Comte, P. Liska, L. Cevey, E. Costa, V. Shklover, L. Spiccia, G. B. Deacon, C. A. Bignozzi, M. Graetzel, *J. Am. Chem. Soc.* **2001**, *123*, 1613–1624; e) M. K. Nazeeruddin, A. Kay, I. Rodicio, R. Humphry-Baker, E. Müller, P. Liska, N. Vlachopoulos, M. Grätzel, *J. Am. Chem. Soc.* **1993**, *115*, 6382–6390; f) C. Klein, M. K. Nazeeruddin, P. Liska, D. Di Censo, N. Hirata, E. Palomares, J. R. Durrant, M. Graetzel, *Inorg. Chem.* **2005**, *44*, 178–180; g) R. Argazzi, C. A. Bignozzi, T. A. Heimer, F. N. Castellano, G. J. Meyer, *J. Am. Chem. Soc.* **1995**, *117*, 11815–11816; h) B. Gholamkhass, K. Koike, N. Negishi, H. Hori, T. Sano, K. Takeuchi, *Inorg. Chem.* **2003**, *42*, 2919–2932.
[4] a) V. Balzani, F. Scandola in *Supramolecular Photochemistry*, Horwood, Chichester, **1991**; b) A. P. de Silva, H. Q. N. Gunaratne, T. Gunnlaugsson, A. J. M. Huxley, C. P. McCoy, J. T. Rademacher, T. E. Rice, *Chem. Rev.* **1997**, *97*, 1515–1566.
[5] a) R. Konduri, H. Ye, F. M. MacDonnell, S. Serroni, S. Campagna, K. Rajeshwar, *Angew. Chem.* **2002**, *41*, 3185–3187; b) M. Kaneko, N. Katakura, C. Harada, Y. Takei, M. Hoshino, *Chem. Commun.* **2005**, *27*, 3436–3438; c) K. Maeda, T. Takata, M. Hara, N. Saito, Y. Inoue, H. Kobayashi, K. Domen, *J. Am. Chem. Soc.* **2005**, *127*, 8286–8287.
[6] S. L. Gilat, S. H. Kawai, J.-M. Lehn, *J. Chem. Soc., Chem. Commun.* **1993**, *18*, 1439–1442.
[7] J.-P. Sauvage, *Acc. Chem. Res.* **1998**, *31*, 611–619.
[8] V. Balzani, S. Campagna, G. Denti, A. Juris, S. Serroni, M. Venturi, *Acc. Chem. Res.* **1998**, *31*, 26–34.
[9] A. Hagfeldt, M. Graetzel, *Acc. Chem. Res.* **2000**, *33*, 269–277.
[10] S. Rau, B. Schäfer, A. Grüßing, S. Schebesta, K. Lamm, J. Vieth, H. Görls, D. Walther, M. Rudolph, U. W. Grummt, E. Birkner, *Inorg. Chim. Acta* **2004**, *357*, 4496–4503.
[11] W. F. Wacholtz, R. A. Auerbach, R. H. Schmehl, *Inorg. Chem.* **1986**, *25*, 227–234.

[12] F. Venema, H. F. M. Nelissen, P. Berthault, N. Birlirakis, A. E. Rowan, M. C. Feiters, R. Nolte, *Chem. Eur. J.* **1998**, *4*, 2237–2250.
[13] A. R. Oki, R. J. Morgan, *Synth. Commun.* **1995**, *25*, 4093–4097.
[14] E. Eskelinen, S. Luukkanen, M. Haukka, M. Ahlgrén, T. A. Pakkanen, *J. Chem. Soc., Dalton Trans.* **2000**, 2745–2752.
[15] A. Ambroise, R. W. Wagner, P. Dharma Rao, J. A. Riggs, P. Hascoat, J. R. Diers, J. Seth, R. K. Lammi, D. F. Bocian, D. Holten, J. S. Lindsey, *Chem. Mater.* **2001**, *13*, 1023–1034.
[16] T. J. Anderson, J. R. Scott, F. Millett, B. Durham, *Inorg. Chem.* **2006**, *45*, 3843–3845.
[17] No detailed discussion of bond length and angles will be presented.
[18] N. Nickita, M. J. Belousoff, A. I. Bhatt, A. M. Bond, G. B. Deacon, G. Gasser, L. Spiccia, *Inorg. Chem.* **2007**, *46*, 8638–8651.
[19] B. Schaefer, H. Goerls, S. Meyer, W. Henry, J. G. Vos, S. Rau, *Eur. J. Inorg. Chem.* **2007**, *25*, 4056–4063.
[20] B. Schäfer, H. Görls, M. Presselt, M. Schmitt, J. Popp, W. Henry, J. G. Vos, S. Rau, *Dalton Trans.* **2006**, 2225–2231.
[21] M. A. Bennett, G. Wilkinson, *Chem. Ind.* **1959**, 1516.
[22] T. B. Hadda, H. Le Bozec, *Polyhedron* **1988**, *7*, 575–577.
[23] K. Wiederholt, L. W. McLaughlin, *Nucleic Acids Res.* **1999**, *27*, 2487–2493.
[24] S. Anderson, E. C. Constable, K. R. Seddon, J. E. Turp, J. E. Baggott, M. J. Pilling, *J. Chem. Soc., Dalton Trans.* **1985**, *11*, 2247–2261.
[25] *COLLECT*, Data Collection Software, Nonius B. V., Netherlands, **1998**.
[26] Z. Otwinowski, W. Minor, "Processing of X-ray Diffraction Data Collected in Oscillation Mode" in *Methods in Enzymology*, vol. 276, Macromolecular Crystallography, Part A (Eds.: C. W. Carter, R. M. Sweet), Academic Press, San Diego, **1997**, pp. 307–326.
[27] *SMART*, Software for the CCD Detector System, version 5.05, Bruker AXS, Madison, WI, **1998**.
[28] G. M. Sheldrick, *Acta Crystallogr., Sect. A* **1990**, *46*, 467–473.
[29] G. M. Sheldrick, *SHELXL-97*, University of Göttingen, Germany, **1993**.

Received: December 3, 2007
Published Online: June 13, 2008

